

# Measurement and Calculation of Diesel Spray Penetration

Hiro Hiroyasu and Haiyan Miao

Kinki University

Diesel spray penetration was investigated by using *light sheet interception* technique. The parameters investigated are: ambient pressure, valve opening pressure, orifice diameter, length-to-diameter ratio and injection pump speed. The results show that the diesel spray penetration is affected greatly by the injected fuel momentum flow rate, nozzle geometry and density of ambient gas. A model to predict the spray penetration after it emerges from the nozzle is also introduced in this paper. This model is applicable to real engine fuel injection systems with varied injection pressures during the diesel injection period. Verified by the measured spray tip penetration, the model provides a useful tool for the investigation of diesel spray related phenomena and for the multi-dimensional diesel engine in-cylinder processes simulations.

## 1. Introduction

Many efforts have been put to meet more and more stringent new emissions regulations, while at the same time enhancing the performance of diesel engines. In small direct injection diesel engines being developed for automotive applications, liquid phase fuel penetration is one of the important factors to optimize the in-cylinder processes. The nozzle introduces and distributes the fuel in such a way that the diesel fuel can be atomized, vaporized and mixed with air effectively in quite limited space of the combustion chamber within milliseconds. Penetration of the liquid phase fuel is necessary to promote fuel-air mixing. But if liquid fuel impinges and collects on the piston head, this phenomenon may lead to higher emissions. Therefore, it is very important to obtain a good understanding of the spray penetration. The knowledge on spray penetration is useful for engine design and the development of computational models used as engine design and optimization tools.

Diesel spray penetration has been studied by many researchers since the beginning of last century. The spatial and temporal characteristics of diesel spray are usually observed and measured <sup>[1-12]</sup>. Many valuable data had been obtained by the photographic techniques as well as the laser techniques. However, by using the photographic techniques, only a limited number of films can be collected for entire injection cycle. It is also time-consuming and costly to process and analyze them. In this paper, a developed convenient technique, which can measure the diesel spray penetration systematically, is described. Based on this technique, the experiments were carried out via wide operation conditions and various nozzle structures. The measured spray penetrations are illustrated and discussed.

Besides the experimental studies, there were many theoretical and empirical correlations recommended for the prediction of spray penetration <sup>[13-24]</sup>. As these correlations were developed for the spray with constant line pressures, more efforts were carried out to include the influence of varied line pressures <sup>[25]</sup>. However, this model failed to describe the spray penetration process in fully mathematic way, which prevents its application for computational models. In this study, more efforts are carried out. A simple spray penetration model for a real fuel injection system is obtained. In this paper, this simple spray penetration model, which is applicable for multi-dimensional diesel engine

in-cylinder process computational models, is introduced and verified by the measured spray penetrations.

## 2. Measurement of Diesel Spray Penetration

In order to measure the tip penetration of diesel sprays systematically, a technique, called the *light sheet interception technique* was developed <sup>[26]</sup>. Several light sheets, each perpendicular to the spray axis, were arranged at different locations downstream of the nozzle. When the spray tip intercepts each of the light sheets, the arrival time of the spray tip can be detected from the attenuation of the transmitted light sheet intensity with a photo detector. Information about the spray structure and the spray tail behavior can also be obtained from the shapes of the deflection signals. After confirming that the light sheet interception method has sufficient accuracy for detecting the arrival of the spray tip, two detectors based on the same principle were applied.

The experimental arrangements are shown schematically in Fig. 1. The detector was installed on the wall of the pressure vessel. The light sheet for each detection unit was emitted from a light emitting diode, and was received by a phototransistor. The space between the light-emitting parts and the receiving parts ran alongside the spray axis. The first light sheet was positioned at the nozzle exit, while the others were set downstream at uneven intervals along the spray axis. The output of the phototransistors, after being amplified, was transferred through an A/D converter into a microcomputer for real-time acquisition. The A/D converter started to convert the analog signals from the ten phototransistors to digital ones after an external trigger signal produced by an electromagnetic pickup mounted near the rotating shaft of the pump just several milliseconds before the start of the injection. The acquisition and the conversion of one datum required 5 $\mu$ s, and the number of digitized data of ten signals for each spray was 4000. The transfer of the converted data from the A/D converter to the computer was pursued simultaneously. Then the fuel was injected into the pressure vessel and its spray intercepted the ten light sheets, and each interception signal was transferred to the computer until the spray tail passed the last light sheet. The data acquisition and conversion was interrupted and waited until the next external trigger. After the A/D converter repeated the data acquisition and conversion for ten successive injection cycles, the data were analyzed. Ten pairs of the spray tip arrival time and the distance from the nozzle to each light sheet were calculated, and therefore, the mean value and the variation of the arrival time of the spray tip at each light sheet were obtained. In this system, the injection characteristics, such as needle lift, injection pressure and injection rate were measured in order to examine the relevance of the injection characteristics to the spray characteristics.

Figure 2 shows an example of the measured results for the ambient pressure of 3 Mpa. Fig. 2(a) shows the output signals from the ten phototransistors. All the signals have clear interception points marked with short vertical lines in the figure. The calculated spray tip penetration via time is drawn in Fig. 2(b). Ten continuous injection cycles were measured. The mean values and the scattering of the spray tip penetration were analyzed, as shown in Fig. 3(a). The experiments were then carried out by using a single-hole injector under different conditions as shown in Table 1.

Table 1 Measurement range and standard operation condition

	Range	Standard condition
Injection pump speeds	from 250 rpm to 1000 rpm	500 rpm
Valve opening pressure	from 10 to 35 MPa	20 MPa
Ambient pressures	from 0.1 to 3 MPa	3 MPa
Injected mass	20 and 35 mg/cycle	20 mg/cycle
Nozzle orifice diameters	0.25 and 0.3 mm	0.3 mm
Length-to-diameter ratios (L/D)	from 2 to 6	4

### 1) Effect of ambient pressures

Figure 3(a) shows that during the early injection period, the penetration increases with time

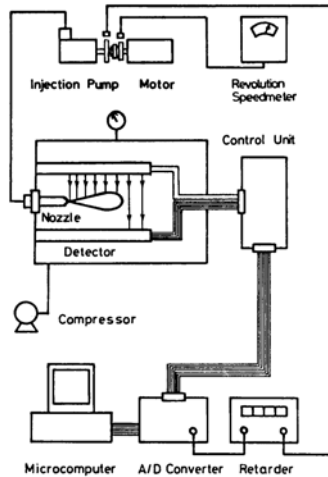


Fig. 1: Schematic experimental apparatus for spray tip penetration measurement

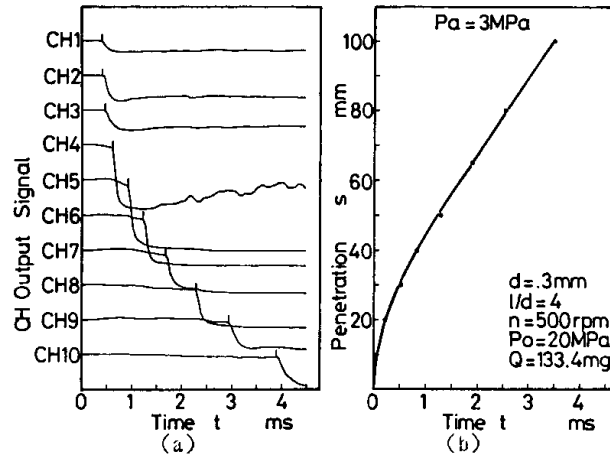


Fig. 2: An example of measured results

acceleratingly due to the initial sharp injection pressure rise and is independent of the ambient pressure until 10 mm downstream of the nozzle. Then by increasing the ambient pressure under same temperature, spray penetration is reduced dramatically. Similar observation results were obtained by Siebers<sup>[12]</sup>, who found that the ambient gas density has a strong non-linear effect on liquid length and as the gas density increases, the liquid length decreases.

## 2) Effect of valve opening pressures

Figure 3(b) and 3(c) were obtained under different ambient pressures of 0.1 Mpa and 3 Mpa respectively. The valve opening pressures were varied from 10 Mpa to 35 Mpa. It was found that the valve opening pressure impacts the spray characteristics to a large extent. A higher valve opening pressure raises injection pressure and injection rate, consequently increases the injection velocity and therefore leads to an increase of the spray penetration. It was also observed that this effect is weakened by increasing ambient pressures. Siebers measured liquid length over higher range from 40 Mpa to 170 Mpa and found that the effect of orifice pressure drop is negligible at this range<sup>[12]</sup>. Therefore, the spray penetration trace with high valve opening pressure (above 40 Mpa) may be very similar to that with 35 Mpa valve opening pressure.

## 3) Effect of length-to-diameter ratios (L/D)

Figure 3(d) and 3(e) show how the length-to-diameter ratios affect spray penetration under different ambient pressures. It is clear that the length-to-diameter ratio does not affect the spray penetration significantly. Observation was made by Siebers with similar conclusions on length-to-diameter ratio effect on the liquid lengths<sup>[12]</sup>.

## 4) Effect of orifice diameters

Figure 3(f) and 3(g) present the measured results conducted with two nozzles of 0.25mm and 0.3mm diameters under different ambient pressures. In Fig. 3(g), the spray penetration from the nozzle of 0.3mm is larger than that from 0.25mm diameter nozzle under 3 Mpa ambient pressure. It is noticed that at 1 ms after start of injection, the distances of spray penetration are almost proportional to their nozzle diameters. Siebers also found this linear relationship based on his experiments taken over the nozzles of 0.1mm, 0.2 mm up to 0.5 mm<sup>[12]</sup>. However, Fig. 3(f) shows no proportional relationship of spray tip penetration under low ambient pressure of 0.1 Mpa. It may be explained in the following way: The injection velocity is reduced by an enlarged orifice nozzle under the same injection pressures. On the other hand, the larger orifice nozzle produces larger droplets, whose momentums are relatively larger than that from a smaller orifice nozzle. At low ambient pressure, the retard force acting on the droplets is small so that the small droplets from smaller orifice nozzle have similar traces with that of the large droplets. Therefore, the spray penetration is similar under low ambient pressure. However, at very high ambient pressures, the spray tip penetration depends on the injected

fuel momentum rather than the fuel injection velocity. Therefore, the spray from larger orifice hole has longer penetration, which is proportional to their nozzle diameters.

### 5) Effect of pump speeds

Figure 3(h) and 3(i) show that the higher the pump speed is, the larger the spray tip penetration is. More detailed discussion was given in <sup>[26]</sup>.

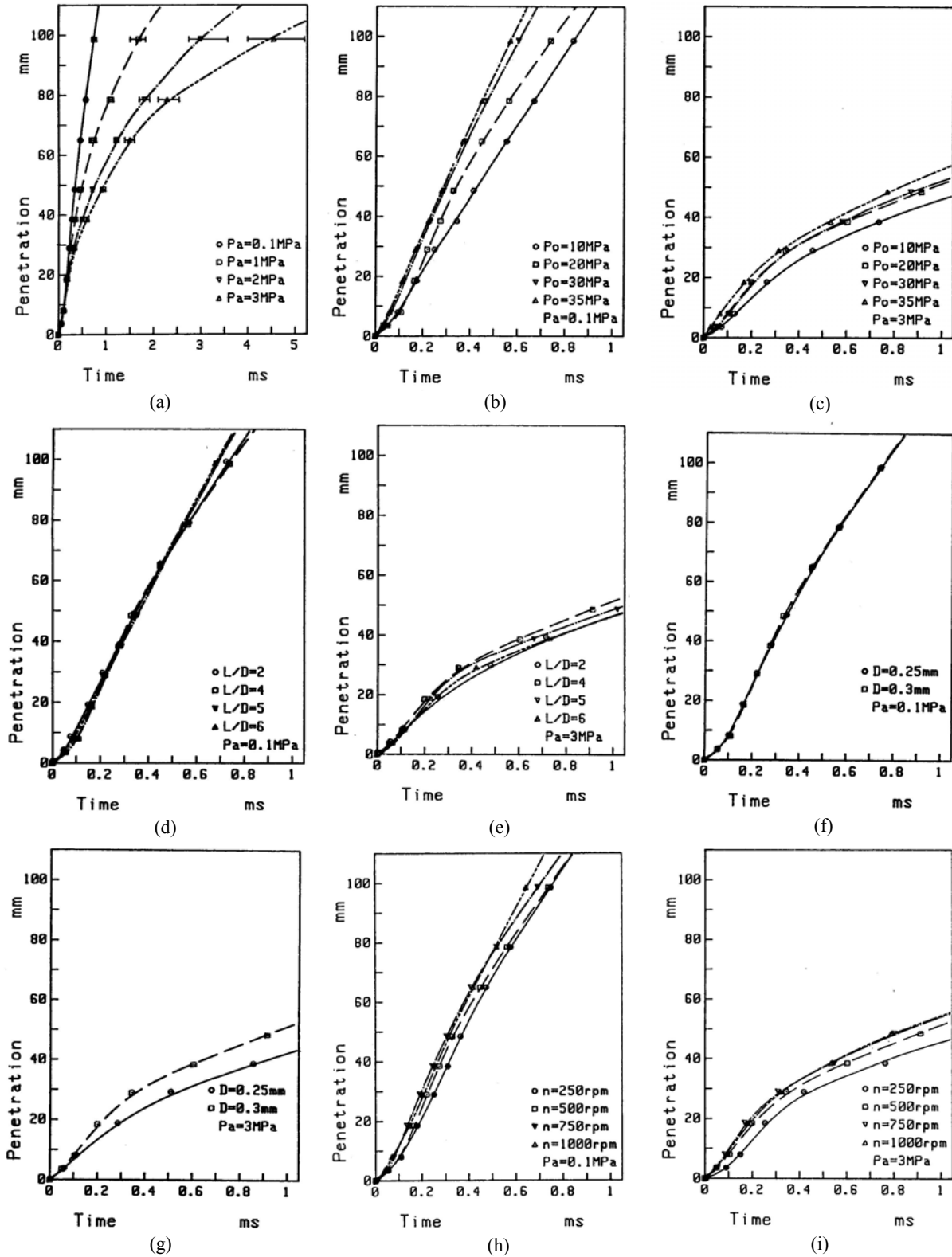


Fig. 3: Effects of operating conditions and nozzle structure on spray penetration

### 3. Calculation of Diesel Spray Penetration

Beside the experimental studies, many theoretical and empirical correlations were recommended for the prediction of diesel spray penetration. Some correlations<sup>[13-17]</sup> showed that spray penetration is in proportion to the square root of time from the start of injection, while others<sup>[18-19]</sup> indicated that center velocity of the fuel spray at the initiation of the injection is constant. A detailed review of these correlations was given by Hiroyasu<sup>[20]</sup>.

As the correlations mentioned above were developed for sprays with constant line pressures, more efforts were carried out to include the influence of varied line pressures<sup>[25]</sup>. A model was developed, which took into account the overtaking phenomenon occurring among the fuel elements. Although the calculated spray tip penetrations were in good agreement with the measured ones, a map of breakup length coefficients was used as a part of the model. This makes the further application of this model into the multi-dimensional diesel spray related combustion models rather difficult.

In this paper, we describe an improved spray tip penetration model that is capable to calculate spray penetration under varied line pressures in a real diesel injection system. A new breakup length correlation obtained from experiment data is used, which make it possible to describe the spray tip penetration injected from a real injection system in the full mathematical way. The model is also validated by the experimental results over a wide range of operating conditions.

#### 3.1 Spray Penetration Correlation Under Constant Line Pressures

Extensive studies of spray tip penetration have been carried out by Hiroyasu et al.<sup>[21-24]</sup>. They found the linear relationship with two different slopes between logarithmic expressions of penetration and time. At the initiation of the injection, the slope was 1, while after a short period of time, the slope changed to 0.5. This indicated that the spray velocity at the initiation of the injection is a constant and then spray penetration is in proportion to the square root of time. Hiroyasu and Arai<sup>[24]</sup> obtained their correlations based on their extensive experimental results with the aid of the jet disintegration theory of Levich<sup>[27]</sup> and the Reichardt's free jet theory<sup>[28]</sup>, as:

$$\begin{aligned} 0 \leq t < t_b : \quad S &= C \sqrt{\frac{2\Delta P}{\rho_a}} t \\ t_b \leq t : \quad S &= \sqrt{\alpha C} \left( \frac{2\Delta P}{\rho_a} \right)^{1/4} \sqrt{D \cdot t} \end{aligned} \quad (1)$$

where C is a coefficient;  $\alpha$ , breakup length coefficient;  $\Delta P$ , pressure drop through the nozzle;  $\rho_a$ , density of gas;  $\rho_l$ , density of liquid fuel; D, orifice diameter and  $t_b$  is determined by

$$t_b = \frac{\alpha}{\sqrt{2} \cdot C} \cdot \frac{\rho_l}{\sqrt{\rho_a}} \cdot \frac{D}{\sqrt{\Delta P}} \quad (2)$$

In Bracco's investigation<sup>[29]</sup>, the breakup length coefficient  $\alpha$  has a value of 7.15, with respect to 15.8 in Hiroyasu and Arai's equation<sup>[24]</sup>. The effects of nozzle hole entrance shape, length-diameter ratio and cavitation number were included into the correlation of the breakup length coefficient  $\alpha$  by Hiroyasu and his coworkers<sup>[24]</sup>. However, the correlation is too complicated to be used easily.

In this study, the measured breakup lengths presented in<sup>[24]</sup> were re-examined carefully seeking for a simple correlation. A new correlation is obtained in form of:

$$L_b = C' \left( \frac{L}{D} \right)^{0.13} \left( \frac{\rho_l}{\rho_a} \right)^{0.5} D \quad (3)$$

where C' is a constant with value of 9.05;  $\rho_l$ , density of liquid fuel;  $\rho_a$ , density of gas; D, orifice diameter; L, length of nozzle. According to the jet disintegration theory of Levich, the breakup length for a real injection system is also determined by

$$L_b = \alpha \sqrt{\frac{\rho_l}{\rho_a}} \cdot D \quad (4)$$

where  $\alpha$  is breakup length coefficient;  $\rho_l$ , density of liquid fuel;  $\rho_a$ , density of surrounding gas; D, orifice diameter; L, length of nozzle. Substituting the Eq. 4 into Eq. 3, the breakup length coefficient is then obtained, as:

$$\alpha = C' \left( \frac{L}{D} \right)^{0.13} \quad (5)$$

In the spray tip penetration model described below, this equation is used to determine the breakup length coefficient for Eq. 1 and 2.

### 3.2 Spray Penetration Model Applicable to Engine Fuel Injection Systems

Spray penetration in a diesel engine is strongly controlled by the transient injection pressures. Assuming that the injection duration is divided into many small time durations, so that the injected diesel can be treated as a fuel element. The fuel element is characterized with different constant line pressures, whose penetration can be determined by the correlations in section 3.1. Therefore, it is possible to apply constant line pressure correlations for the calculation of spray penetration from real injection systems. This model is explained through a sample calculation as below.

- (i) Divide the injection period equally into a great number of short time intervals of 0.015 ms in order to obtain the spray penetration with the transiently varied injection pressure history like Fig. 4. Take the transient value of the injection pressure at the middle of each intervals as the representative injection pressure, and time at the start of the interval as the representative injection time for the fuel element involved in this interval.
- (ii) Calculate the trajectory of each fuel element by applying the correlations under constant line pressures described in the section 3.1. In this study, coefficient  $C$  and constant  $C'$  are valued 0.9 and 9.05 respectively. Figure 5 schematically illustrates the trajectories of the fuel elements (a-k), which correspond to the elements with short time interval shown in Fig. 4. Note: For a clear demonstration, the time interval for each element in Fig. 4 and 5 is much larger than the actual calculation.
- (iii) Compare the trajectories among all elements. At each time step, take the fuel element whose trajectory is the furthest away from the nozzle as the spray penetration at that instant. However, its successive trajectory after this moment should be excluded in the follow comparisons. This is due to the fact that once a fuel element reaches the spray tip, it is directly exposed in the surrounding air and hence receives a much bigger drag than when it moves inside the spray. The fuel element is then overtaken immediately by the other fuel elements. Accordingly, the overtakes among the fuel elements injected at different times are supposed to occur frequently at the spray tip, and no fuel element can exist at the spray tip except for a very short period.
- (iv) As the result of the comparisons, the line covering all the trajectories represents the diesel spray penetration. It is noticeable that the overtakes between trajectories of the fuel elements in Fig. 5 are correspondent very well with their transient injection pressures shown in Fig. 4.

The model is verified by comparing the calculated spray penetration with the measured ones. In Fig. 6-8, symbols  $\square$ ,  $*$ ,  $\Delta$ ,  $\diamond$ , represent the experimental results under different operating conditions with ambient pressure of 0.1 Mpa, 1 Mpa, 2 Mpa and 3 Mpa respectively. The solid lines in Fig. 6-8 show the calculated results under the same conditions of the corresponding symbols. As shown in Fig. 6-8, the calculated results match very well with the measured penetrations over wide operation conditions.

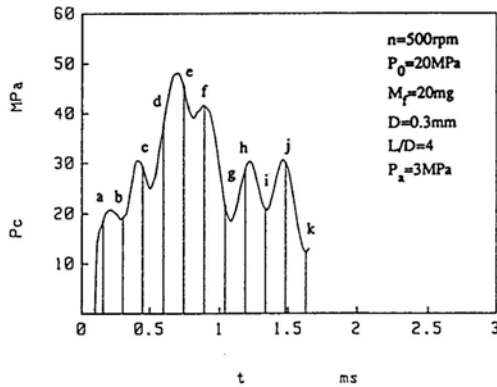


Fig. 4: Illustration of division of injection pressure history into elements with short time interval

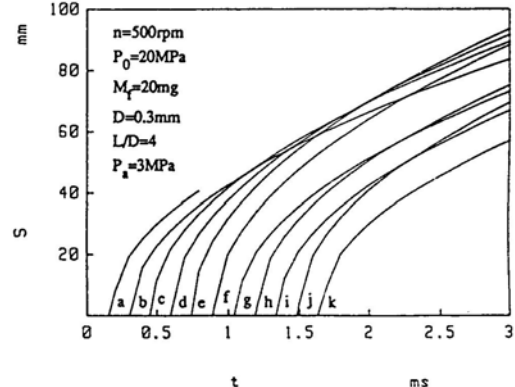
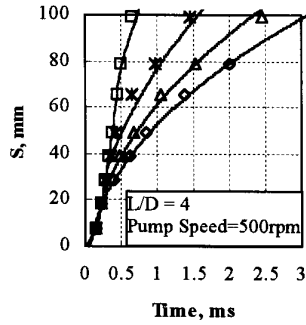
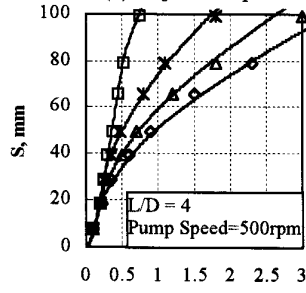


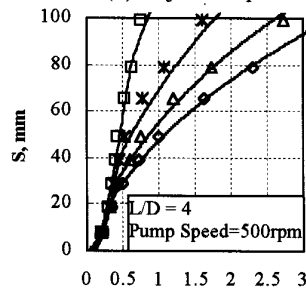
Fig. 5: Trajectories of fuel elements a-k illustrated in Fig. 4



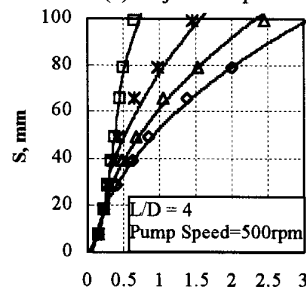
(a)  $P_{inj} = 10$  Mpa



(b)  $P_{inj} = 20$  Mpa

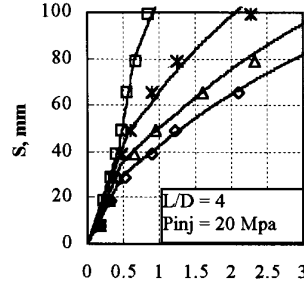


(c)  $P_{inj} = 30$  Mpa

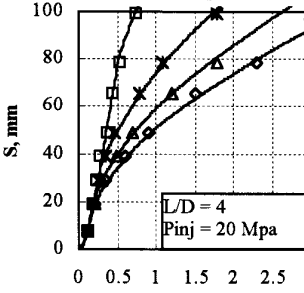


(d)  $P_{inj} = 35$  Mpa

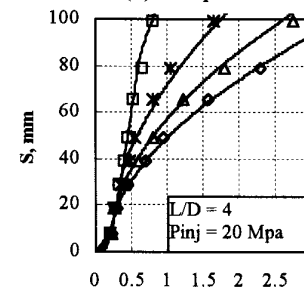
Fig. 6: Measured and calculated spray penetration at various ambient gas and injection pressures



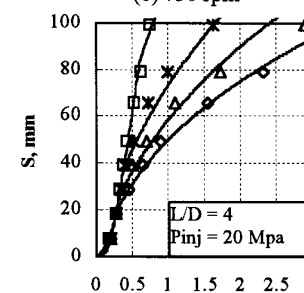
(a) 250 rpm



(b) 500 rpm

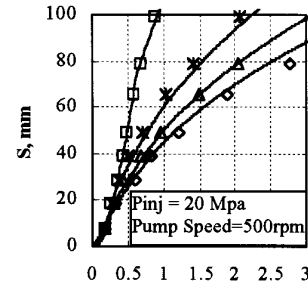


(c) 750 rpm

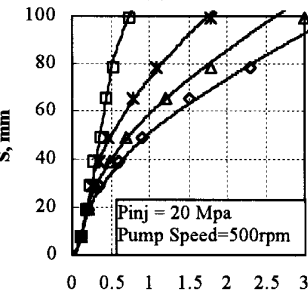


(d) 1000 rpm

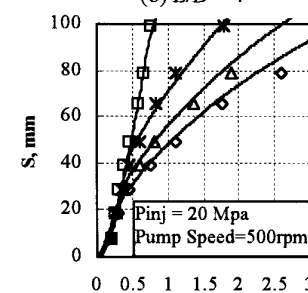
Fig. 7: Measured and calculated spray penetration at various pump speeds and ambient gas pressures



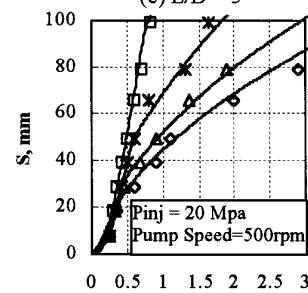
(a)  $L/D = 2$



(b)  $L/D = 4$



(c)  $L/D = 5$



(d)  $L/D = 6$

Fig. 8: Measured and calculated spray penetration of various nozzle structures

Note: This correlation is verified by the experimental results with injection pressures under 35 Mpa. According to the experimental results by Siebers<sup>[12]</sup>, the effect of injection pressures on liquid length in a diesel spray is negligible over a injection pressure range from 40 Mpa up to 170 Mpa. This observation suggests that the breakup length correlation and the spray penetration model obtained in this research are applicable to higher injection pressures. This simple model can be an effective tool for predicting the spray penetration in diesel engines, which will be useful in multi-dimensional engine in-cylinder process simulation and understanding of the transient characteristics of diesel sprays.

#### 4. Conclusion

By using the *light sheet interception* technique, the effects of the operating conditions and nozzle geometry on diesel spray penetration were investigated. The observations show that during the early injection period, the penetration increases with time acceleratingly. Spray penetration is reduced dramatically with the increased ambient pressures and increased by a higher valve opening pressures. Length-to-diameter ratio does not affect the spray penetration significantly. The effect of nozzle diameters is dependent on the ambient pressures. A new diesel spray penetration correlation was introduced in the form of

$$0 \leq t < t_b : \quad S = C \sqrt{\frac{2\Delta P}{\rho_l}} t$$

$$t_b \leq t : \quad S = \sqrt{\alpha C} \left( \frac{2\Delta P}{\rho_a} \right)^{1/4} \sqrt{D \cdot t}$$

with  $\alpha$  and  $t_b$  being determined by

$$\alpha = C' \left( \frac{L}{D} \right)^{0.13} \quad t_b = \frac{\alpha}{\sqrt{2} \cdot C} \cdot \frac{\rho_l}{\sqrt{\rho_a}} \cdot \frac{D}{\sqrt{\Delta P}}$$

where  $\alpha$ ; breakup length coefficient;  $C$  is a coefficient valued of 0.9;  $C'$ , a constant with value of 9.05;  $\Delta P$ , pressure drop through the nozzle;  $\rho_a$ , density of gas;  $\rho_l$ , density of liquid fuel;  $D$ , orifice diameter and  $L$ , length of nozzle. It was applied in the spray tip penetration model for engine fuel injection systems and validated by experimental results over a wide range operating conditions.

#### Acknowledgements

This work was supported by Japanese Science Promotion Society (JSPS).

#### References

- [1] Hiroyasu H and Arai M 1978 *Trans. JSME*, **34**-385, 3208
- [2] Varde K S and Popa D M 1983 *SAE paper* 830448
- [3] Yule A L, Mo S L, Tham S Y and Aral S M 1985 *ICLASS-85*, Paper IIB/2/1
- [4] Browne K R, Partridge I M and Greeves G 1986 *SAE paper* 860223
- [5] Kamimoto T, Yokota H and Kobayashi H 1987 *Transactions of the SAE*, **96**-4, 783-91
- [6] Arcoumanis C, Cossali E, Paal G and Whitelaw J H 1989 *SAE paper* 890314
- [7] Hodges J T, Baritaud T A and Heinze T A *Transactions of the SAE* 1991 **100**-3 1284-302
- [8] Bower G R and Foster D E 1993 *SAE paper* 930864
- [9] Yeh C N, Kamimoto T, Kobori S and Kosaka H 1993 *SAE paper* 932652
- [10] Espey C and Dec J E 1995 *Transactions of the SAE* **104**-4 1400-14
- [11] Naber J D and Siebers D L 1996 *Transactions of the SAE* **105**-3 82-111
- [12] Siebers D L 1998 *SAE paper* 980809
- [13] Schweitzer P H 1938 *J. of Applied Physics* **9**-12 735
- [14] Parks M V, Polonski C and Toye P 1966 *SAE paper* 660747
- [15] Wakuri Y, Fujii M, Amitani T and Tsuneya R 1960 *Bull. of JSME*, **3**-9 123
- [16] Dent J C 1971 *SAE paper* 710571
- [17] Hay H and Jones P L 1972 *SAE paper* 720776
- [18] Rife J and Heywood J B 1974 *SAE paper* 740948
- [19] Reitz R D 1978 *PhD thesis* Princeton University
- [20] Hiroyasu H 1985 *Proceedings of the International Symposium on Diagnostics and Modeling of Combustion in Reciprocating Engine* 53-75
- [21] Hiroyasu H, Takahashi N and Takahashi M 1968 *Paper of JSME* **201** 101
- [22] Hiroyasu H, Kadota T and Yokoyama Y 1974 *Bull. of Faculty of Eng., Hiroshima University*, **23**-1 55
- [23] Hiroyasu H, Kadota T and Tasaka S 1978 *Trans. of JSME* **44**-385 3208
- [24] Hiroyasu H and Arai M 1980 *Trans of JSME* **21** 5; 1990 *SAE Paper* 900475
- [25] Xu M, Nishida K and Hiroyasu H 1992 *SAE paper* 920624
- [26] Xu M and Hiroyasu H 1990 *SAE paper* 902077
- [27] Levich V G 1962 *Physicochemical Hydrodynamics* Prentice-Hall Inc. 639
- [28] Reichardt H 1941 *Z. A. M. M. Bd.* **21**:5 257
- [29] Bracco F V et al 1985 *SAE paper* 850126